Materials Science and Engineering A 468–470 (2007) 184–192

MATERIALS SCIENCE & ENGINEERING A

www.elsevier.com/locate/msea

Damage mechanisms of cast Al–Si–Mg alloys under superimposed thermal–mechanical fatigue and high-cycle fatigue loading

Tilmann Beck *, Detlef Löhe, Jochen Luft, Ingo Henne

Institut für Werkstoffkunde I, Universität Karlsruhe (TH), Kaiserstr. 12, D-76128 Karlsruhe, Germany

Received 31 March 2006; received in revised form 27 May 2006; accepted 31 May 2006

Abstract

Out-of-phase thermal–mechanical fatigue (TMF) tests with superimposed higher frequency mechanical fatigue (HCF) loading were performed at three cast Al–Si cylinder head alloys. All materials show for maximum temperatures of the TMF cycle between 200 and 250 °C a threshold of the amplitude of the superimposed HCF loading below of which the number of TMF cycles to failure is not significantly affected by the superimposed HCF loading. Above this threshold the TMF life shows a strong decrease with increasing HCF loading. Extensive microscopic analyses revealed that independent from the HCF loading first cracks are initiated at eutectic Si-particles detached from the surrounding α-Al matrix. Crack propagation occurs at small HCF amplitudes along the eutectic regions. At higher superimposed HCF loadings an accelerated crack propagation along slip bands within the α-Al matrix is observed.
© 2007 Elsevier B.V. All rights reserved.

Keywords: Thermal–mechanical fatigue; High-cycle fatigue; Cast aluminium alloys; Damage behaviour

1. Introduction

Cast aluminium alloys used for cylinder heads, engine blocks and pistons of turbocharged diesel engines are subjected to complex thermal and mechanical loadings [1,2]. On the one hand, the inhomogeneous and time-dependent temperature profiles during start–stop processes lead to a thermally induced fatigue loading with low frequency and, especially in the "hot" regions of the components, large plastic strain amplitudes. This kind of service loading can be simulated at uniaxially loaded specimens by thermal–mechanical fatigue (TMF) testing. In the recent decades, a remarkable amount of experimental work has been carried out on TMF of this class of alloys [3–10].

On the other hand, the combustion pressure and oscillating masses result in a mechanical fatigue loading with relatively high frequency and distinctly smaller strain amplitudes than induced by the thermal fatigue cycles. There is even a bigger amount of materials data from isothermal high-cycle fatigue (HCF) testing on typical cast aluminium alloys used for engine applications than from TMF loading [11–17].

However, there are currently few first results about the lifetime and damage behaviour of aluminium alloys under combined low frequency TMF loadings superimposed with higher frequency mechanical HCF loadings. Results from tests under such TMF/HCF loadings on Ni-base sheet alloys showed that linear damage accumulation hypotheses are not applicable under such combined loadings [18]. First results obtained at cast aluminium alloys resulted in a similar finding [19,20]. However, there is a great lack of experimental data from TMF/HCF loading at cast aluminium alloys and the respective damage and failure mechanisms are up to now just qualitatively understood.

In order to analyze the synergy of damage caused by the low frequency thermal and the higher frequency mechanical loading and to get quantitative fatigue life data under such loading conditions, superimposed TMF/HCF tests at the cylinder head alloys AlSi7Mg, AlSi5Cu3 and AlSi10Mg (numbers indicate wt.%) were conducted in total strain control. The tests were performed with and without dwell times t_d at the maximum temperature T_{max}, different values of T_{max}, several mechanical strain amplitudes $\varepsilon_{a,t}^{me}$(TMF) and for superimposed TMF/HCF loading $\varepsilon_{a,t}^{me}$(HCF) with frequencies between 5 and 20 Hz.

The results are comprehensively presented as lifetime diagrams. Furthermore, extensive metallographic investigations and scanning electron microscopy (SEM) studies of the crack initiation and propagation process are shown which allow for

* Corresponding author. Tel.: +49 721 608 4159; fax: +49 721 608 8044.
E-mail address: tilmann.beck@mach.uni-karlsruhe.de (T. Beck).

0921-5093/$ – see front matter © 2007 Elsevier B.V. All rights reserved.
doi:10.1016/j.msea.2006.05.177

Table 1
Heat treatment of the three investigated aluminium alloys

	AlSi7Mg-T6	AlSi5Cu3-T7	AlSi10Mg-T6
Annealing	5 h at 525 °C	10 h at 495 °C	4 h at 525 °C
Quenching medium/ temperature	Water/20 °C	Water/20 °C	Water/50 °C
Ageing	8 h at 160 °C	4 h at 210 °C	8 h at 180 °C

a clear identification of the crack initiation and propagation mechanisms under TMF/HCF loading.

2. Experimental details

2.1. Test material

TMF and superimposed TMF/HCF-testing was performed at the cast aluminium alloys AlSi10Mg and AlSi7Mg, both in the peak hardened (T6) state. A further set of tests was made at AlSi5Cu3 in a slightly overaged state (T7). The dendrite arm spacing of all materials was about 40 μm. The parameters of heat treatment are given in Table 1. Metallographic images of the three alloys are shown in Fig. 1. For fatigue testing round solid specimens were machined with a gage diameter of 7 mm, a parallel length of 20 mm and a gage length of 15 mm. The specimen shoulders had a diameter of 12 mm.

2.2. Test setup

The TMF tests without superimposed HCF loading were performed on an electromechanical test rig with 100 kN maximum load. The computerized control unit allows to switch from force to strain control during a running test. For strain measurement, a water-cooled capacitive high temperature extensometer was applied. Force was measured by the built-in load cell of the testing machine. The specimen was heated by a 5 kW induction generator operating at a frequency of about 200 kHz. Cooling was achieved by heat conduction to the water-cooled fixtures and additionally by three air jets blowing radial to the surface of the test piece. For temperature, closed loop control was achieved by a digital process controller. The setpoints for temperature and mechanical loading were generated by a PC-based system which also performed the data acquisition with about 1000 measured values per cycle. For superimposed TMF/HCF testing the same test setup with a servohydraulic test rig was used.

2.3. Test conditions

The temperature cycles of the TMF tests had a minimum temperature of 50 °C and heating and cooling ramps with 10 K/s for all tests. Due to the high thermal conductivity of the investigated alloys, the radial temperature differences are estimated to be smaller than 5 °C. The maximum temperature T_{max} was varied between 200 and 300 °C in steps of 25 °C. Dwell times t_d at T_{max} between 0 s (triangular T–t cycle) and 180 s were applied. At the beginning of each test five reference cycles at zero stress were performed to establish a dynamic thermal equilibrium in the test rig and to measure the thermal strain ε^{th} as a function of time and temperature. Afterwards, the machine was switched to total strain control. Then the thermal strain was in most of the tests totally suppressed (total strain ε_t = constant) such that

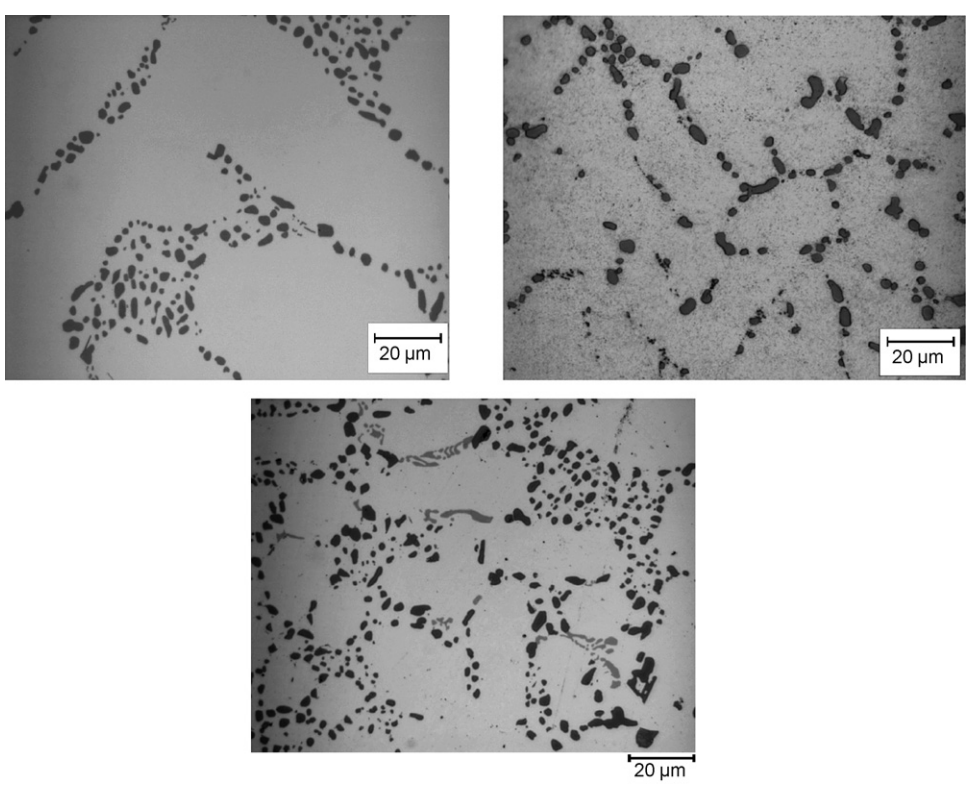

Fig. 1. Microstructure of AlSi7Mg (top left), AlSi5Cu3 (top right) and AlSi10Mg-T6 (bottom) in the as-received state.

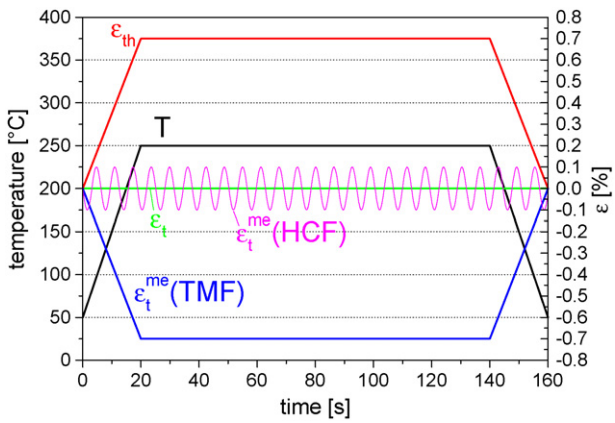

Fig. 2. Temperature- and strain-time paths for TMF and TMF/HCF.

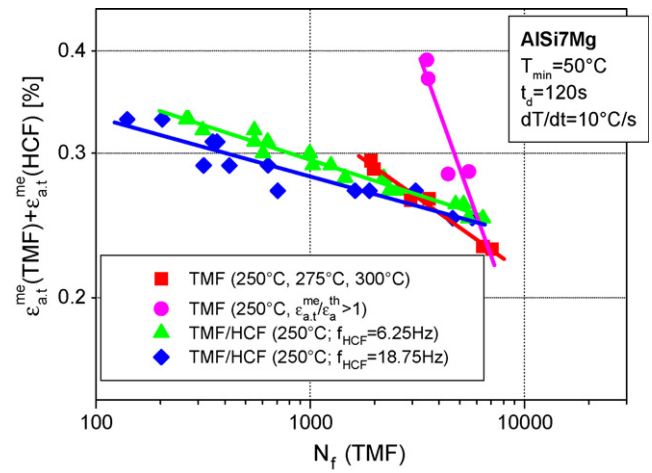

Fig. 3. Lifetime behaviour of AlSi7Mg at TMF and TMF/HCF loading.

the total mechanical strain ε_t^{me} was, according to the condition $\varepsilon_t = \varepsilon^{th} + \varepsilon_t^{me}$, phase shifted by 180° against the temperature (out-of-phase TMF) and had the same amplitude as the thermal strain. In some tests a ε_t-time cycle with compressive peak strains was applied in order to receive out-of-phase TMF loading with mechanical strain amplitudes larger than the thermal strain amplitude.

The HCF loading was also applied in total strain control and directly superimposed to the ε_t-time path of the TMF cycle and therefore also superimposed to the total mechanical strain of the TMF cycle. For the HCF loading, frequencies of $f_{HCF} = 6.25$–18.75 Hz were applied. The amplitudes $\varepsilon_{a,t}^{me}$(HCF) were varied between 0.02% and 0.1% and were therefore significantly lower than the mechanical strain amplitudes from TMF loading $\varepsilon_{a,t}^{me}$(TMF) which ranged from 0.2% to 0.4%. The temperature-, ε_t-, ε^{th}-, and ε_t^{me}-time paths are schematically drawn in Fig. 2.

The tests were stopped at an ultimate number of TMF cycles of 10^4 or when the specimen failed by fracture. Some tests were interrupted after defined numbers of cycles and the surface was examined by confocal white light microscopy and SEM. After failure metallographic examination of the microstructure was performed.

3. Results and discussion

3.1. Lifetime behaviour of AlSi7Mg and AlSi5Cu4

The lifetime behaviour of AlSi7Mg under pure TMF and superimposed TMF/HCF loadings is shown in Fig. 3, where the sum of the total mechanical strain amplitude from TMF cycling $\varepsilon_{a,t}^{me}$(TMF) and the superimposed HCF-strain amplitude $\varepsilon_{a,t}^{me}$(HCF) are plotted versus the number of TMF cycles to failure. The corresponding results from AlSi5Cu3 are given in Fig. 4. All tests were conducted with a dwell time of 120 s at maximum temperature. Pure TMF tests were on the one hand conducted with $T_{max} = 250$, 275 and 300 °C and total constraint of the thermal strain ($\varepsilon_{a,t}^{me}$(TMF) $= \varepsilon_a^{th}$). These results are given by squares. On the other hand, at $T_{max} = 250$ °C, $\varepsilon_{a,t}^{me}$(TMF) was varied to values larger than the thermal strain amplitude in order to specify the influence of mechanical loading on the lifetime at a given maximum temperature (circles). The results from TMF/HCF testing at $T_{max} = 250$ °C, TMF cycles with total strain constraint and an HCF frequency of 6.25 Hz are given by triangular symbols. The corresponding results from $f_{HCF} = 18.75$ Hz are represented by diamonds.

Under pure TMF loading the lifetime of both materials decreases more pronounced if $\varepsilon_{a,t}^{me}$ is risen together with T_{max} in the condition $\varepsilon_{a,t}^{me} = \varepsilon_a^{th}$ than with increasing $\varepsilon_{a,t}^{me}$(TMF) at a constant maximum temperature of 250 °C. The difference between the slope of the resulting strain–life curves is bigger for AlSi7Mg than for AlSi5Cu3. Superimposed HCF loadings up to $\varepsilon_{a,t}^{me}$(HCF) = 0.02% result for both materials and HCF frequencies only in a weak decrease of TMF lifetime. The respective data points lie on the same line as the results for pure TMF loading at $T_{max} = 250$ °C and $\varepsilon_{a,t}^{me} > \varepsilon_a^{th}$. However, at HCF amplitudes above 0.02% a steep decrease of lifetime with increasing $\varepsilon_{a,t}^{me}$(HCF) is observed which is the more pronounced the higher the frequency of the HCF loading is. It should be remarked that the fatigue limit of AlSi7Mg for strain controlled isothermal fatigue at temperatures between 20 and 250 °C is above 0.06% [21] which means that superimposed HCF loadings clearly below the fatigue limit strongly affect the TMF life.

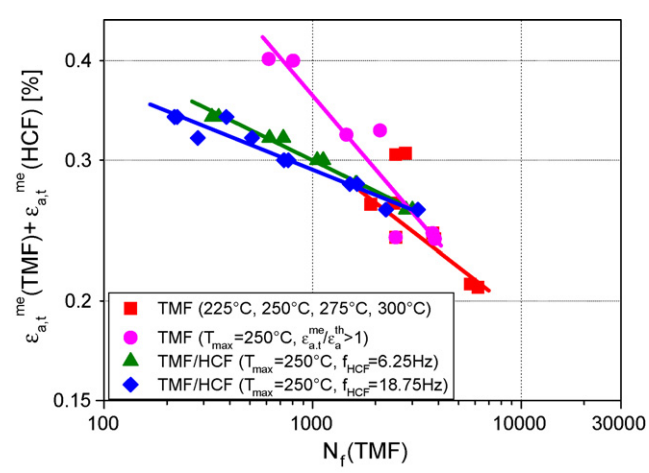

Fig. 4. Lifetime behaviour of AlSi5Cu3 at TMF and TMF/HCF loading.

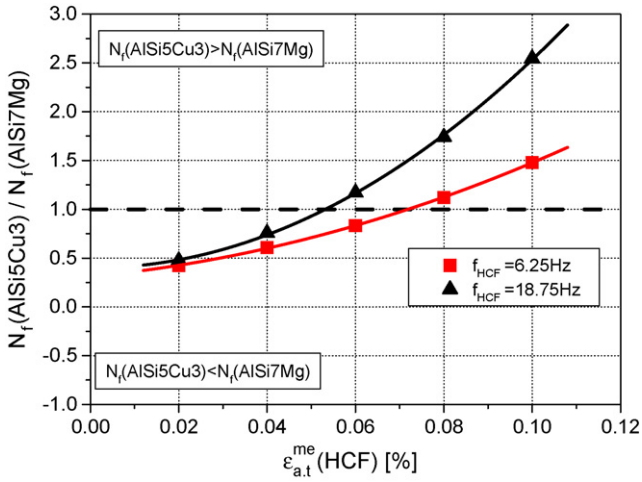

Fig. 5. Ratio of TMF life of AlSi7Mg and AlSi5Cu3 under TMF/HCF loading.

It is concluded that for both materials and $T_{max} = 250\,°C$ a threshold value of $\varepsilon^{me}_{a,t}$(HCF) exists, below of which the superimposed HCF loading just results in the same small decrease of lifetime as is effected by an increment of $\varepsilon^{me}_{a,t}$(TMF) of 0.02%. Above this threshold, obviously a strong synergy of damage induced by the TMF and the HCF loading exists which leads to a very steep decrease of the TMF lifetime. Further investigations at the same materials revealed that a similar threshold behaviour is observed at $T_{max} = 225\,°C$ [21].

Fig. 5 gives a comparative view on the lifetime behaviour of AlSi7Mg and AlSi5Cu3 under superimposed TMF/HCF loading by plotting the ratio of the TMF cycles to failure of these materials versus $\varepsilon^{me}_{a,t}$(HCF) for both investigated f_{HCF}. Up to the threshold value of $\varepsilon^{me}_{a,t}(HCF) = 0.02\%$, which is identical for both materials, the lifetime of AlSi5Cu3 is just about half of the lifetime of AlSi7Mg. This is caused by the higher peak stresses occurring at AlSi5Cu3 due to the less-pronounced loss of strength by overageing compared to AlSi7Mg. However, with increasing HCF loading the difference between the TMF lifetimes of both materials decreases and at the largest $\varepsilon^{me}_{a,t}$(HCF) AlSi5Cu3 reaches higher lifetimes than AlSi7Mg. As expected, this behaviour is the more pronounced the higher f_{HCF} is. Obviously, the higher strength of AlSi5Cu3 at elevated temperatures and the smaller amount of overageing which results in the relatively low lifetimes under pure TMF loading, leads to the lower sensitivity on superimposed HCF loadings.

3.2. Crack initiation and propagation in AlSi7Mg under TMF and TMF/HCF loading

It is assumed that the strong decrease of TMF lifetime by superimposed HCF loadings with amplitudes above 0.02% is caused by the following damage processes:

- The cyclic deformation behaviour and especially the amount of plastic deformation before first cracks are formed are mainly determined by the TMF cycle, whereas the HCF loading results, due to its small amplitude and high frequency, in nearly elastic deformation.
- The plastic strain amplitude and the peak stress induced by the TMF cycle determine the number of cycles to crack initiation.
- The crack propagation is mainly determined by the superimposed HCF loading. Obviously, even small $\varepsilon^{me}_{a,t}$(HCF), which still lie below the fatigue limit at isothermal loading, result in a strong increase of the crack propagation rate.

To investigate the damage mechanisms and to prove the assumptions made above, optical and scanning electron microscopy of the specimen surface after TMF and TMF/HCF loading and of the microstructure within the gage section was performed.

Fig. 6 shows the crack initiation and propagation of AlSi7Mg under pure TMF loading with $\varepsilon^{me}_{a,t}(TMF) = \varepsilon^{th}_{a}$ and $T_{max} = 250\,°C$. In the left picture, a crack initiated at an eutectic Si-particle detached from the surrounding α-Al matrix can be seen. The picture on the right hand side shows macrocracks solely propagating along the eutectic regions. The crack initiation at detached Si-particles is caused by the thermal and mechanical misfit of these brittle components of the microstructure with respect to the surrounding ductile matrix. Crack propagation is characterised by the connection of such microcracks in the eutectic regions of the microstructure.

Fig. 7 shows optical micrographs of longitudinal sections of the gage lengths. In the left picture, the situation after TMF loading with the same conditions as in Fig. 6 and in the right picture after TMF/HCF loading with $\varepsilon^{me}_{a,t}(HCF) = 0.08\%$ is presented. The special etching procedure according to Weck and Leistner [22] visualize the fatigue-induced slip bands. It becomes obvious that the density of these slip bands is distinctly higher in the case of TMF/HCF loading than under pure TMF with the same temperature cycle and mechanical strain amplitude.

This increasing density of fatigue slip bands with increasing $\varepsilon^{me}_{a,t}$(HCF) has a strong influence on crack propagation: As becomes obvious from Fig. 8 and from the SEM pictures discussed in the following paragraph which give evidence of crack propagation along slip bands through the α-Al matrix, this kind of crack propagation is only observed at superimposed TMF/HCF loading with $\varepsilon^{me}_{a,t}(HCF) > 0.02\%$ and is therefore obviously responsible for the strong decrease of TMF life with increasing superimposed HCF loading.

Starting from these results, a more detailed study of crack initiation and propagation has been performed at the cylinder head alloy AlSi10Mg in a later research project. The key results of this work are given in the following section.

3.3. Lifetime and damage behaviour of AlSi10Mg under superimposed TMF/HCF loading

The influence of superimposed HCF loadings with $\varepsilon^{me}_{a,t}(HCF) = 0.02\%$ up to 0.08% and a frequency of 5 Hz on the TMF life of AlSi10Mg in the T6 state is given in Fig. 9. In all tests a maximum temperature of $T_{max} = 250\,°C$ was applied and the thermal expansion was completely suppressed throughout the TMF-cycle ($\varepsilon^{me}_{a,t}(TMF) = \varepsilon^{th}_{a}$). The minimum temperature was 50 °C. Results of tests without dwell time at T_{max} are rep-

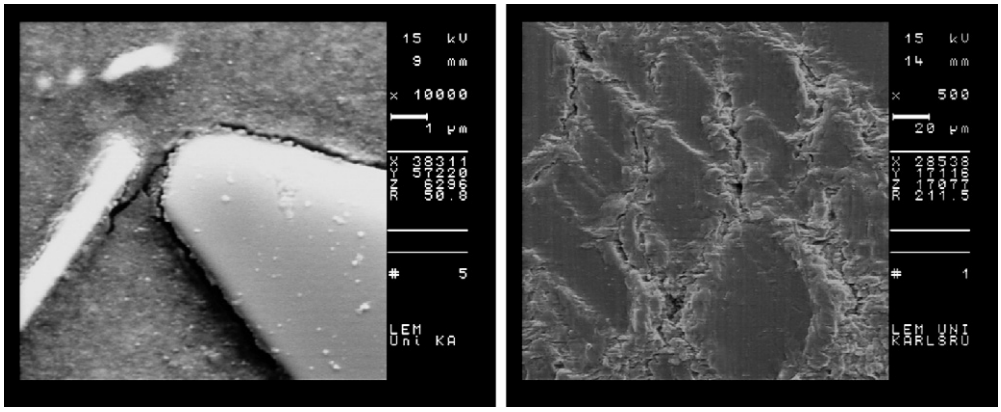

Fig. 6. Crack initiation and propagation in AlSi7Mg under TMF loading with $\varepsilon_{a,t}^{me}(\text{TMF}) = \varepsilon_a^{th}$ and $T_{max} = 250\,°C$.

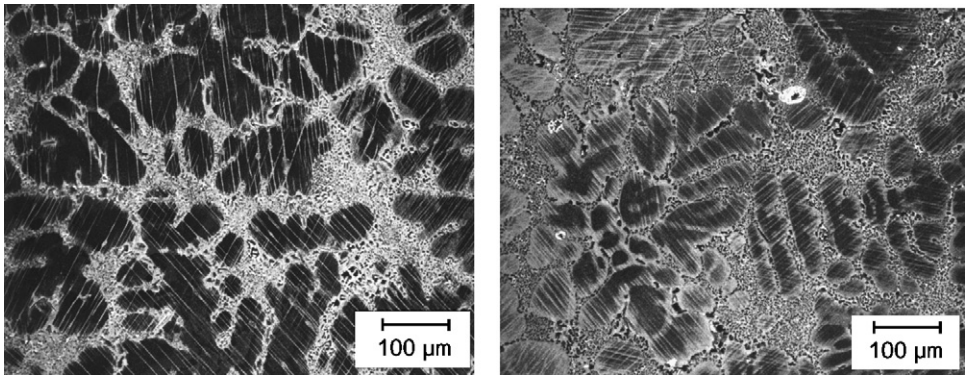

Fig. 7. Fatigue slip bands in AlSi7Mg after TMF loading ($\varepsilon_{a,t}^{me}(\text{TMF}) = \varepsilon_a^{th}$; $T_{max} = 250\,°C$, left) and after TMF/HCF loading ($\varepsilon_{a,t}^{me}(\text{HCF}) = 0.08\%$, right).

resented by squares, those with a dwell time of $t_d = 180$ s by triangles. Open symbols indicate TMF tests without superimposed HCF loading, full symbols TMF/HCF tests. TMF tests without dwell time reach the ultimate number of cycles of 10^4, for $t_d = 180$ s the lifetime is about 7000 cycles. In both cases increasing superimposed HCF amplitudes lead to a significant decrease of lifetime which is more pronounced for TMF/HCF tests with dwell time, because in this case there is a higher number of superimposed HCF cycles per TMF cycle. For $t_d = 180$ s a similar threshold value of $\varepsilon_{a,t}^{me}(\text{HCF})$, below of which the TMF life is almost not affected by the superimposed HCF loading, is observed as at AlSi7Mg and AlSi5Cu3.

To get a deeper understanding of crack initiation and propagation, TMF and TMF/HCF tests were conducted with different T_{max}, dwell times and superimposed HCF loadings on specimens with an initially polished surface. The tests were interrupted after 1, 10, 100, 1000 cycles and after $N \approx N_f/2$ to investigate the specimen's surface with a confocal white light microscope and in

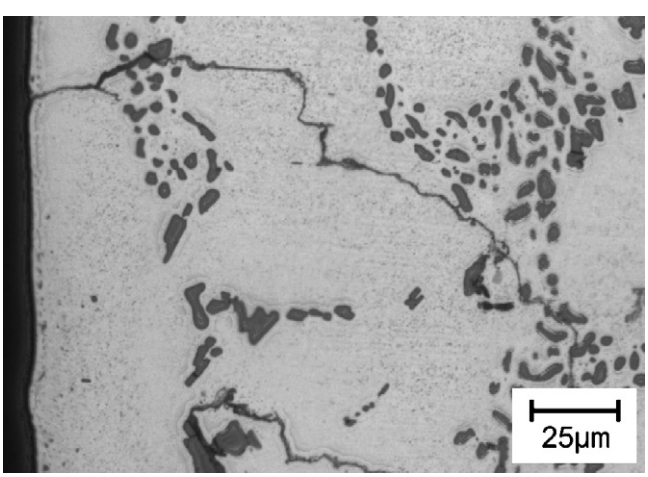

Fig. 8. Crack propagation along fatigue slip bands in AlSi7Mg under TMF/HCF loading with $\varepsilon_{a,t}^{me} = 0.08\%$.

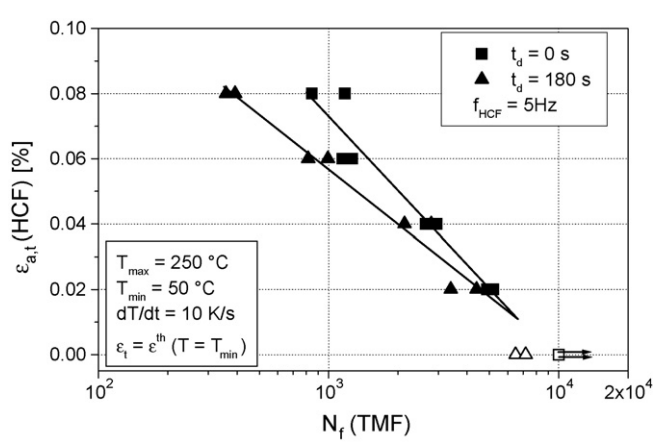

Fig. 9. Influence of superimposed HCF loading on the TMF life of AlSi10Mg.

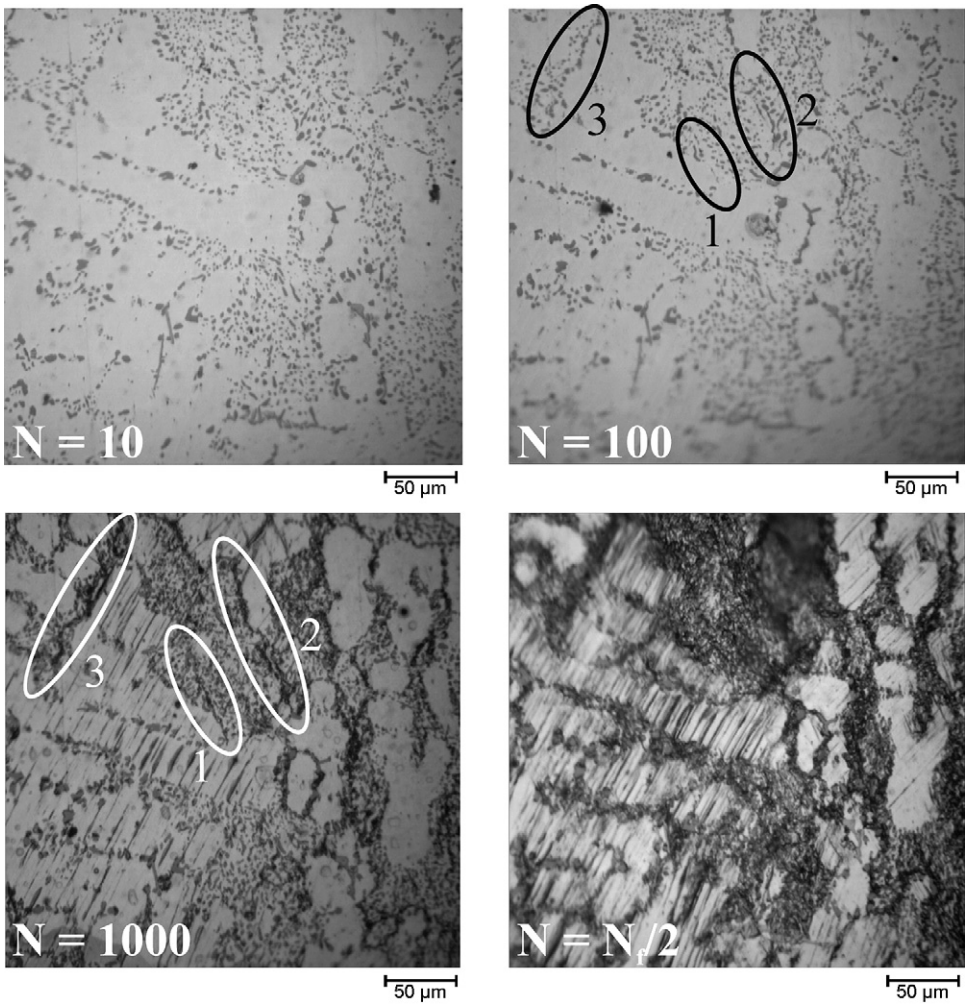

Fig. 10. Development of the surface of AlSi10Mg during TMF with $T_{max} = 250\,°C$.

special cases with SEM. In the following pictures the direction of loading is always horizontal, otherwise it is indicated by an arrow.

Fig. 10 shows surface micrographs of the same position within the gauge length after $N = 10$, 100, 1000 and $N_f/2$ TMF cycles with $T_{max} = 250\,°C$ and $t_d = 0\,s$. First damage can be detected after 100 cycles where cracks of about 50 µm length appear in the eutectic regions (positions 1 and 2) and the interface between the primary α-Al crystals and the eutectic zones (position 3). The cracks propagate significantly until $N = 1000$. At the surface, silicon particles located in the crack path are detached from the α-Al matrix and then passed by the crack. However, in metallographic cross-sections also broken Si-particles are found. This can be attributed to the fact that at the surface biaxial stresses arise in the vicinity of the eutectic Si-particles that cause yielding of the α-Al matrix and thus a separation from the silicon particles, whereas in the interior of the specimen a triaxial stress state with high normal stresses results in particle rupture. Furthermore, after $N = 1000$ slip bands within the primary α-Al as well as distinctive plastic deformation appear at the surface. After $N \approx N_f/2$ cycles the slip band formation in the primary α-Al and the plastic deformation in the eutectic regions is such pronounced that the initially detected cracks cannot be seen anymore. This dramatic change of the surface topography especially in the eutectic regions is illustrated by the SEM image after $N = N_f/2$ in Fig. 11 and results from the differences of the

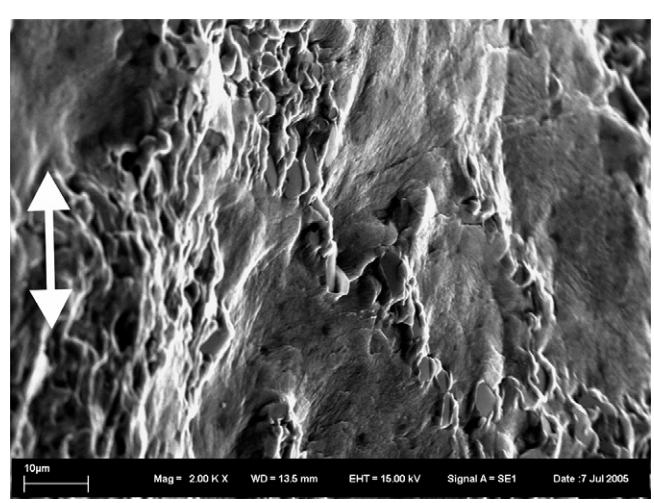

Fig. 11. SEM image of AlSi10Mg after 3450 TMF cycles with $T_{max} = 250\,°C$.

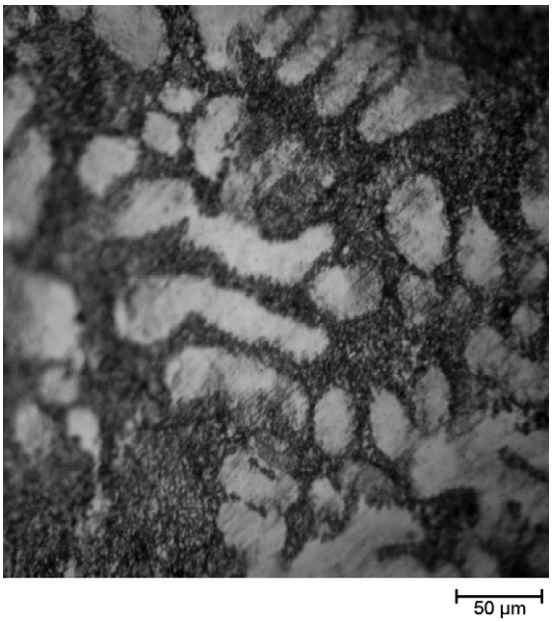

Fig. 12. Surface of AlSi10Mg after 1000 TMF cycles with $t_d = 180$ s.

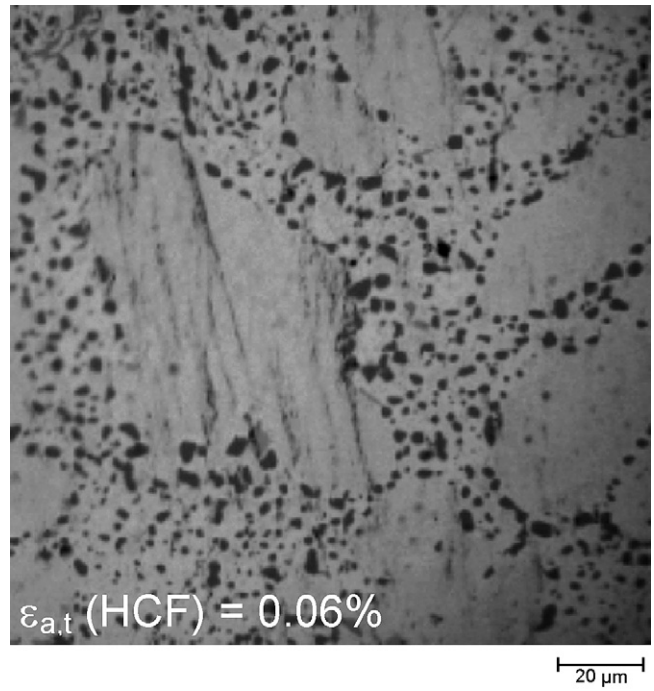

Fig. 13. Surface of AlSi10Mg after 100 cycles of TMF/HCF loading with $T_{max} = 250\,°C$ and $t_d = 180$ s.

thermal expansion coefficient, the strength and Youngs modulus between the α-Al matrix and the eutectic Si-particles.

Fig. 12 shows the surface topography after 1000 TMF cycles with $T_{max} = 250\,°C$ and a dwell time of 180 s on. With increasing dwell time overageing of the initially T6 hardened material becomes more pronounced and the stress relaxation during t_d induces additional plastic deformation. Consequently, a distinctly rougher surface topography results than at $t_d = 0$s. Whilst the several silicon particles within the eutectic region still can clearly be seen after testing without dwell time (see Fig. 10), the eutectic region appears as a homogeneously rough area after TMF with $t_d = 180$ s.

A typical surface after TMF with superimposed HCF loading is shown in Fig. 13. Whereas no slip bands appear within the primary α-Al crystals after 100 TMF cycles without HCF at $T_{max} = 250\,°C$ (see Fig. 10), slip bands can be detected after the same number of TMF cycles with superimposed HCF load-

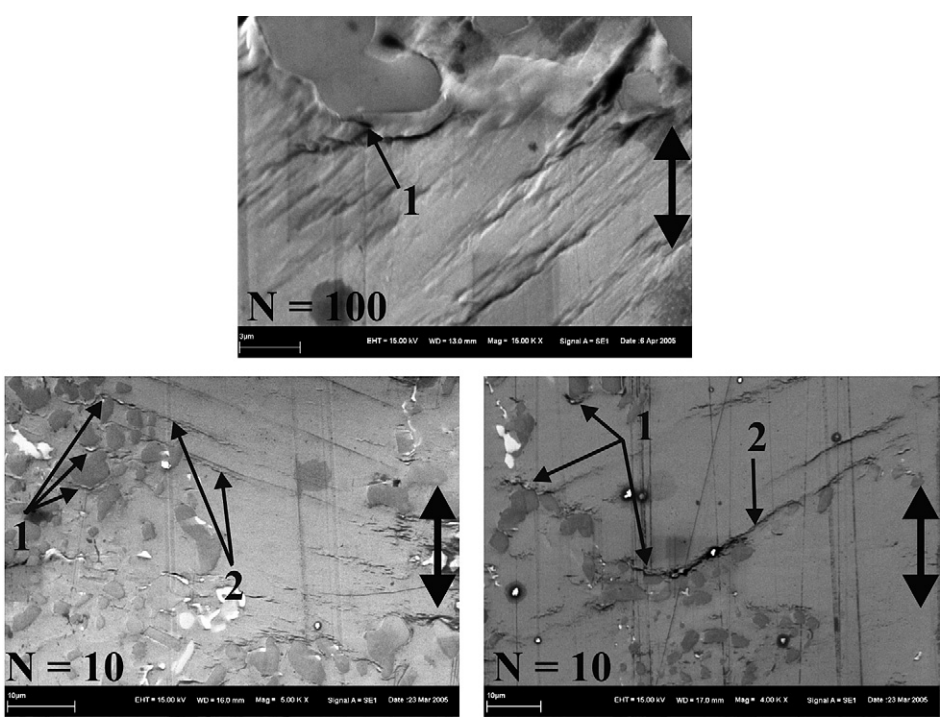

Fig. 14. SEM images of AlSi10Mg after 10 and 100 TMF/HCF cycles at $T_{max} = 300\,°C$, $t_d = 180$ s and $\varepsilon_{a,t}$ (HCF) = 0.06%.

ing with $\varepsilon_{a,t}^{me}(HCF) = 0.06\%$. The influence of superimposed HCF loadings on the formation of slip bands is even more pronounced at $T_{max} = 300\,°C$ where after 10 cycles of TMF/HCF loading with $\varepsilon_{a,t}^{me}(HCF) = 0.06\%$ first slip bands are observed [21]. On the one hand this dependence of the damage behaviour on T_{max} can be attributed to the fact that $\varepsilon_{a,t}^{me}(TMF)$ increases with T_{max} in the case of TMF testing with fully constrained thermal expansion. On the other hand the stronger overageing with increasing temperature leads to a significant reduction of strength and therefore facilitates cyclic plastic deformation during the superimposed HCF cycles.

The SEM pictures after 10 and 100 cycles of TMF/HCF loading with $T_{max} = 300\,°C$ $t_d = 180\,s$ and $\varepsilon_{a,t}^{me}(HCF) = 0.06\%$ in Fig. 14 give a detailed insight to the interaction of TMF- and HCF-induced damage. The strong plastic deformations resulting from the TMF cycles lead to a separation of silicon particles from the α-Al matrix (position 1). Such detached Si-particles were generally found to be the sites of crack initiation, independent of T_{max}, t_d and $\varepsilon_{a,t}^{me}(HCF)$. This gives evidence that superimposed HCF-amplitudes give – if any – a negligible contribution to crack intiation. Starting from detached Si-particles, the cracks either propagate along slip bands through primary α-Al crystals (position 2) or at the interface between primary α-Al crystal and eutectic regions (position 3). Because superimposed HCF loadings increase the quantity of slip bands, crack propagation along slip bands becomes more dominant with increasing $\varepsilon_{a,t}^{me}(HCF)$.

4. Conclusions and outlook

In order to analyze the synergy of damage caused by superimposed low frequency thermal and high-frequency mechanical loading and to get quantitative fatigue life data under such loading conditions, superimposed thermal–mechanical fatigue (TMF)/high-cycle fatigue (HCF) tests at the cylinder head alloys AlSi7Mg, AlSi5Cu4 and AlSi10Mg were conducted in total strain control. Out-of-phase TMF loadings with different mechanical strain amplitudes were applied with a dwell time of $t_d = 0$–$180\,s$ at different maximum temperatures and several HCF loadings $\varepsilon_{a,t}^{me}(HCF)$ with frequencies between 5 and 20 Hz were superimposed. In all cases, up to a threshold of $\varepsilon_{a,t}^{me}(HCF) = 0.02\%$ the superimposed HCF loading does not reduce TMF lifetime significantly. However, at $\varepsilon_{a,t}^{me}(HCF) > 0.02\%$ a pronounced decrease of TMF lifetime is caused by superimposed HCF which is the more pronounced the higher the HCF amplitude and the HCF frequency is.

Extensive metallographic investigations and SEM studies of the crack initiation and propagation process were conducted. Under TMF as well as under TMF/HCF loading, crack initiation generally takes place at the interface between eutectic Si-particles and α-Al matrix. Under pure TMF conditions, the cracks propagate solely along the eutectic regions whereas with increasing superimposed HCF loading crack propagation along slip bands within the primary α-Al crystals becomes more dominant.

From this it is concluded that the following damage processes occur in TMF and TMF/HCF loading, respectively:

- Cyclic deformation and crack initiation are mainly governed by the TMF cycle which induces large plastic deformations. The plastic strain amplitude and the peak stress induced by the TMF cycle determine the number of cycles to crack initiation. The superimposed HCF loading results, due to its small amplitude and high frequency, in nearly elastic deformation and therefore has no significant influence on the first states of damage.
- Crack propagation is mainly determined by the superimposed HCF loading. Obviously, even small $\varepsilon_{a,t}^{me}(HCF)$, which still lie below the fatigue limit at isothermal loading, result in a strong increase of the crack propagation rate.

Further research on superimposed TMF/HCF loading of cast aluminium alloys will address the following topics:

- Quantitative description and modelling of the influence of superimposed HCF loadings on TMF life by fracture mechanic approaches.
- Fatigue crack propagation experiments at variable temperature and mean stress in order to quantify the behaviour of HCF-induced fatigue cracks under the conditions of superimposed TMF/HCF loading.
- Detailed investigation of the crack initiation mechanism, especially the stress state and dislocation structure at the interface between eutectic α-Al matrix and Si-particles.

Acknowledgements

The authors thank the Bundesministerium für Bildung und Forschung, the Forschungsvereinigung Verbrennungskraftmaschinen and the Arbeitsgemeinschaft Industrieller Forschungsvereinigungen for the financial support of the presented research.

References

[1] F. Langmayr, F. Zieher, VDI-Ber. 1813 (2004) 227–243.
[2] J. Hadler, S. Flor, C. Heikel, VDI-Ber. 1830 (2005) 285–308.
[3] H. Ikuno, S. Iwanaga, Y. Awano, ASTM STP 1371 (2000) 138–149.
[4] B. Flaig, K.-H. Lang, T. Beck, D. Löhe, E. Macherauch (Eds.), Proceedings of ICAA-6, Toyohashi, 1998, pp. 1397–1402.
[5] H. Sehitoglu, C.C. Engler-Pinto, H.J. Maier, T. Foglesong, in: Proceedings of the CAMP2002, Paderborn/Germany, pp. 76–83.
[6] H. Sehitoglu, T.J. Smith, H.J. Maier, ASTM STP 1371 (2002).
[7] T. Beck, K.-H. Lang, D. Löhe, Mater. Sci. Eng. 319–321 (2002) 662–666.
[8] R.B. Gundlach, B. Ross, A. Hetke, S. Valtierra, J.F. Mojica, Trans. AFS 102 (1994) 205–223.
[9] M. Riedler, W. Eichsleder (Eds.), Proceedings of LCF5, Berlin, 2003, pp. 225–230.
[10] M. Riedler, R. Minichmayr, W. Eichsleder (Eds.), Proceedings of ICF-11, Torino, Italy, 2005 (CD-ROM Edition).
[11] O. Madelaine-Dupich, J. Stolarz (Eds.), Proceedings of the ICAA-5, Grenoble, France, 1996, pp. 1343–1348.
[12] Q.C. Wang, C.H. Caceres, Mater. Sci. Eng. 234–236 (1997) 106–109.
[13] B. Flaig, PhD thesis, Universität Karlsruhe (TH), 1995.
[14] Q. Yao, T. Kobayashi, H. Toda, S. Kitaoka, Proceedings of the ICAA-6, 1998, pp. 1389–1394.
[15] C.M. Styles, P.A.S. Reed, Proceedings of the ICAA-7, Chalottesville, USA, 2000, pp. 1458–1462.

[16] D.L. McDowell, K. Fall, M.F. Horstenmeyer, J. Fan, Eng. Fract. Mech. 70 (2003) 49–80.
[17] S. Nishido, M. Kaneso, T. Kobayashi, H. Toda, Int. J. Cast Met. Res. 17 (2004) 345–350.
[18] J. Luft, T. Beck, D. Löhe, Proceedings of the ICF-11, Torino, Italy, 2005 (CD-ROM Edition).
[19] M. Moalla, PhD Thesis, Universität Karlsruhe (TH), 2004.
[20] T. Beck, R. Ratchev, M. Moalla, K.-H. Lang, D. Löhe, in: L. Remy, J. Petit (Eds.), Temperature–Fatigue Interaction, ESIS–Elsevier, 2002, pp. 115–124.
[21] J. Luft, T. Beck, D. Löhe, Final Report of BMBF Projet 03N3095E.
[22] E. Weck:, E. Leistner, Metallographische Anleitung zum Farbätzen nach dem Tauchverfahren, Deutscher Verlag für Schweißtechnik, 1986, Band 3.